Controls on the phosphorus content of fine stream bed sediments in agricultural headwater catchments at the landscape-scale

B. G. Rawlins[a]

[a]*British Geological Survey, Keyworth, Nottingham NG12 5GG, UK*

Correspondence: B. G. Rawlins. E-mail: bgr@bgs.ac.uk

ABSTRACT

There have been no landscape-scale assessments which quantify the relative importance of the organic and mineral properties of BS (bed sediment) and associated catchment characteristics (geology, land cover and mean topsoil phosphorus (P) content) for BSP concentration. Mid infra red diffuse reflectance spectrometry was applied to estimate the quantities of organic matter, dithionite extractable aluminium- (Al_d) and iron (Fe_d), kaolinite, dioctahedral clay and mica (D&M) minerals in 1052 snapshot samples of fine ($< 150\ \mu$m) BS in small to medium-sized (5-55 km^2) agricultural headwater catchments across a large area (15 400 km^2) of central England. Analyses included estimates of BS specific surface area, cerium (Ce) concentrations (enriched in P-bearing apatite and P-fertilsers), and catchment average topsoil P content.

Simple linear regression demonstrated that the proportion of variance in BSP explained by specific components of BS across all catchments declined in the following order: $Al_d > Fe_d >$ topsoil P = kaolinite = residual iron > organic matter = Ce > D&M > mineral SSA. No single component accounted for more than 36% of the variance in BSP. Multiple regression – including a classification of bedrock lithology and proportions of arable and grassland by area – accounted for 61.9% of the variance in BSP. The proportions of arable and grassland by area in each catchment were statistically significant but the coefficients – negative and positive, respectively – were counter-intuitive. Across this large region – with widely differing geology and soils – Fe_d in BS is more strongly associated with kaolinite than D&M minerals because iron-oxyhydroxides and kaolinite form contemporaneously during pedogenesis. The SSA of fine bed sediments is largely determined by catchment area, fitted accurately using a power function.

1. Introduction

The dominant factors which control dissolved phosphorus (P) concentrations in headwater streams are the quantities and types of P in their bed sediments (BS; House, 2003; van der Perk et al., 2006). Agricultural land use has been identified as a source of enhanced inputs of particulate P (PP) to headwater bed sediments (Withers et al., 2001) which can lead to elevated levels of dissolved P with profound implications for water quality (Smith, 2003).

Transport and delivery of P to headwater sediments in agricultural catchments is complex. There are differing diffuse and point sources which follow varying pathways (erosive inputs, drains, bank slip) and delivery mechanisms (Beven et al., 2005). The largest concentrations of P typically occur in the finer fractions of BS (Evans et al., 2004) because they contain material with the largest P sorption capacities. Much is known about the forms of PP (organic and inorganic) in soils and bed sediments and chemical associations of inorganic P with specific mineral phases. For example, adsorption and occlusion by Al and Fe oxyhydroxides (Hartikainen et al., 2010) , specific and non-specific adsorption on clay minerals (Edzwald et al., 1976) and precipitation as iron-phosphate phases (Emerson and Widmer, 1978), the occurrence of P in rare earth element (REE) enriched apatite (Starinsky et al., 1982) or phosphate fertilisers (Abdel-Haleem et al., 2001), or co-precipitation of phosphorus with calcite (Koschel et al., 1978). The importance of these associations has been demonstrated in selected catchments (e.g. Ballantine et al., 2009; Evans et al., 2004; Palmer-Felgate et al., 2009) but their relative importance is hard to assess because of landscape-scale variations in soil mineralogy (e.g. iron and aluminium oxyhydroxide and clay mineral composition), land use and management, geomorphology and geology. The latter – along with hydrology – was identified as playing an important role in determining spatial and temporal variation in storage of bed sediment P (Ballantine et al., 2009). In their study, Palmer-Felgate et al. (2009) reported higher concentrations of bed sediment phosphorus (BSP) at sites with the greatest agricultural impact across three, paired

headwater catchments in lowland England. No studies to date have investigated the quantities of the different forms of P stored in bed sediment at larger, landscape scales.

One larger scale study (van der Perk et al., 2007) assessed the relative importance of a range of BS element concentrations to explain variations in total bed sediment P in headwaters of the moderate-sized (976 km^2) Tamar catchment (SW England). They showed that the total concentrations of five elements (Al, Fe, K,Ca and Mn) in fine BS collected during the summer months accounted for 32% of BSP, but they did not attempt to identify either the organic matter content or specific mineral phases in their sediment samples. In the research described here, inferences are made regarding the association between BSP and specific components of fine BS based on the amounts of variation accounted for in the former by the latter. For example, much P is occluded within the structures of iron-oxyhydroxides and P is also a constituent of organic matter in sediment. So although these species (e.g Fe-oxyhydroxide occluded P) are not measured directly, their presence is inferred because they account for the variation in BSP. This approach can contribute to our understanding of the processes which determine P delivery to BS and could help to enhance process-based models of sediment P delivery to stream channels (e.g. Davison et al., 2007).

An improved understanding of the importance of the associations of P with specific organic and mineral components in BS samples can be captured by combining the use of landscape-scale, snapshot sediment surveys (Johnson et al., 2005) with mid infra red diffuse reflectance spectrometry (MIR-DRS). Analysis of sediments by MIR-DRS is a rapid and cost-effective technique to accurately estimate the concentrations of several important BS constituents. This technique is particularly effective in circumstances where mineral phases are both amorphous and crystalline. Diffuse reflectance spectrometry has been widely applied in soil science, but less so in the analysis of fluvial sediments (Bertaux et al., 1998; Martinez-Carreras et al.,2010). For accurate quantification, some phases require statistical models to be developed between primary measurements on sediment samples and their spectra before the models can be used

to estimate concentrations of these properties in a larger number of samples. In their study, Martinez-Carreras et al. used the visible and near infra region, but more accurate estimates of specific soil phases are often observed using the mid infra portion of the spectrum (Madari et al., 2006).

Another property of sediments which may influence total P concentrations is the specific surface area (SSA) of its mineral phases. In this paper, the term SSA is used to denote measurements based on the BET isotherm (nitrogen adsorption) which accounts for the surface texture and internal surfaces of certain mineral phases. This is different to estimates of surface area (SA) based on particle size analyses with assumptions regarding particle sphericity. No significant relationships between total P and surface area measured in fine ($<63\mu$m) BS were reported for the Tern, Pang and Lambourn catchments in the UK (Ballantine et al., 2009), nor between SSA and total P for the Enborne catchment (Evans et al., 2004), but a significant positive correlation was reported between SSA and P in the Lambourn (Evans et al., 2004). Although measurements of SSA tend to be relatively costly, Rawlins et al. (2010) recently showed how accurate estimates of mineral SSA of fine BS (following removal of organic matter) could be made from the concentrations of four elements for a large area of central England.

In this paper, statistical analyses are presented showing the relative importance of ten components of fine BS and three catchment features which account for variations in total BSP from 1052 headwater catchments for an area of 15 400 km^2 across central England dominated by agricultural land use. Quantitative estimates of specific BS components include organic matter, mineral SSA, dithionite extractable aluminium- (Al_d) and iron-oxyhydroxides (Fe_d), residual iron, kaolinite and dioctahedral clay and mica (D&M) minerals. A series of catchment-specific features are also included in the statistical analysis: the variation in mean topsoil P concentrations, dominant lithology and the proportions of arable and grassland. The quantities of organic matter, Al_d, and Fe_d were estimated accurately from statistical models developed between primary

measurements and MIR spectra, whilst the relative amounts of kaolinite and D&M minerals in each BS sample were estimated from unique adsorption features. The relationship between mineral SSA and headwater catchment area (5-55 km^2) is also investigated. The implications of the findings from this study for understanding P storage in BS and for modelling the processes governing the transfer of P from soil to aquatic ecosystems are discussed.

2. Study region and methods

2.1. *Geology, soils and land use.*

Bedrock in the study region ranges in age from Precambrian to Cretaceous with a wide range of predominantly sedimentary lithologies including limestones, sandstones, siltstones, mudstones, shale, coal measures, marls, ironstones and chalk (Figure 1). There are also extensive superficial deposits including glacial tills, glacial sands and gravels, marine and river alluvium, river terrace deposits, and to the east of the region, peat deposits (Sylvester-Bradley and Ford, 1968). The soils are dominated by Brown Earths, Surface Water Gleys, Pelosols, Ground Water Gley Soils (Soil Survey of England and Wales, 1983a; Soil Survey of England and Wales, 1983b). The elevation range across the region is between 20 and 255 m above sea level, with undulating topography; the mean slope angle is around 2.5 °. The proportions of land use types across the entire study region are arable (48%), grassland (21%), built-up areas (13%), woodland (7%) and small areas of a range of other land use types (11%.)

2.2. *Bed sediment and topsoil surveys*

Figure 2 shows features of the study region – which covers around 15 400 km^2 of central England – from which selected stream sediments samples were collected. The stream sediment samples were collected by the G-BASE project of the British Geological Survey (Johnson et al., 2005). The stream sediment sampling was undertaken in the summers of 1997, 1998 and 1999 in rural and peri-urban areas.

Potential stream sampling sites were identified using Ordnance Survey maps.

Mainly first and second order streams were selected, either avoiding or located upstream of obvious sources of contamination such as road intersections and farm buildings. Where possible, sediment was collected from central areas of active stream beds after removal of the upper layer of oxidised sediment. Between 15 and 25 kg of sediment was wet-screened on site to collect the fraction finer than 150μm typically yielding a final mineral mass of approximately 500 g. The finer than 150μm fraction was in part chosen because it was shown to be most effective in discriminating between major and trace element bed sediment geochemistry based on orientation surveys (Plant, 1971). All samples were returned to a local field base for air-drying. The location of each stream bed sampling site was recorded using a handheld GPS with an accuracy of around 5 m. At site, the width of each stream, stream order and a classification of flow conditions during sampling were recorded.

In total there were 5047 (not shown) stream sediment sampling sites across the study region. The sites comprise a range of : i) stream orders (1st to 4th), ii) flow conditions (no flow to bank full), and iii) stream channel sizes (widths of a few feet to several metres). We wished to make comparisons of fine BS for streams of similar sizes and flow conditions to avoid any bias such variation might introduce into our analysis. We therefore restricted the number of stream sediment sampling sites to: i) first and second order streams, ii) low to moderate flow conditions, and iii) streams with channels of between 1 and 3 metres width. Of the original 5047 stream sediment sites, a total of 1972 sites met these conditions. Of these sites, a total of 1052 were in catchments where the bedrock geology was sufficiently widespread to form the dominant lithology (see below) in at least 10 catchments across the study region.

Topsoil sampling sites were chosen from alternate kilometre squares across the study area chosen by simple random selection within each square, subject to the avoidance of roads, tracks, railways, urban land and other seriously disturbed ground. At each site, surface litter was removed and soil was sampled to a depth of 15 cm using five holes at the corners and centre of a square with a side of length 20 m by a

hand auger and combined to form a bulked sample. All samples of soil were dried and disaggregated and passed through a sieve (2 mm).

On return to the laboratory, all topsoil and BS samples were coned and quartered and a 50-g sub-sample was ground in an agate planetary ball mill.

2.3. *Chemical analysis and estimation of specific surface area*

2.3.1. *Sediment geochemistry and specific surface area*

The total concentrations of a range of major (including Al, Fe, K, Ca, P and Mn) and trace (including cerium (Ce), Lanthanum (La), molybdenum (Mo), vanadium (V) and rubidium (Rb)) elements were determined in each BS and topsoil sample by wavelength and energy dispersive X-ray fluorescence spectrometry (XRFS). Specific surface area based on nitrogen adsorption was determined on a subset of 60 samples after removal of organic matter. These 60 samples were selected by maximizing the range of total Al concentrations, whilst maintaining a random component in the selection. All samples were prepared using a Micromeritics Gemini VacPrep Degasser; the samples were degassed overnight at 60 °C prior to SSA analysis. The BET specific surface area of each sample was determined using a multi pressure point analysis using a Micromeritics (Norcross, GA, USA) Gemini VI 2385C series physisorption system. A carbon black standard was analysed with each batch of samples to monitor accuracy and precision. With the exception of BS samples with the largest Mo concentrations, Rawlins et al., (2010) showed that SSA in BS from the study region could be accurately estimated for all samples using the total concentration of four elements (V, Al, Rb, and Ca) in a subset of 56 samples by multiple linear regression. This regression model was applied to the data to estimate mineral SSA at the selected sites (n=1052; section 2.2).

2.3.2. *Extraction of iron and aluminium oxyhydroxides*

The 60 samples which had been selected for SSA determination were also used for the determination of dithionite extractable iron (Fe_d) and aluminium (Al_d) oxyhydroxide concentration. In common with other extractants, dithionite is non-specific; it extracts

into solution a range of soil constituents, but dominantly iron oxyhydroxides. Although dithionite is not used routinely as an extractant for aluminium, it has been shown to extract large quantities of non-crystalline aluminium phases from soils (Bera et al., 2005). A mass of approximately 1 g of ground material was weighed using a calibrated balance – the mass recorded – and placed into a 30 ml centrifuge tube. To this, 20 ml of 25% (w/v) sodium citrate ($Na_3C_6H_5O_7.2H_2O$) and 5 ml of 10 % (w/v) sodium dithionite ($Na_2S_2O_4$) was added. The solutions were shaken overnight on a bench-top shaking table and centrifuged the following day at 1370 ***g*** for 4 minutes. A 10 ml aliquot of solution was taken and the concentrations of total iron and aluminum were determined by ICP-AES using matched standard and solution matrices. The concentrations were converted into mass equivalents of Fe_d and Al_d (mg kg^{-1}).

2.3.3. *Total organic carbon*

Total organic carbon was determined for a total of 88 bed sediment samples; the 60 samples referred to above and a further 28 samples; their locations are shown in Figure 2. A 300 mg sub-sample was treated with a small quantity of HCl (5.7 M) to remove any inorganic carbon and total organic carbon was estimated on the remaining sample by combustion in a Costech ECS4010 Elemental Analyser (EA) calibrated against an Acetanilide standard. Replicate analysis of well-mixed samples indicated a precision of $\pm < 0.1\%$. In terrestrial sediments and soils, organic carbon comprises close to 50% of the mass of organic matter (Prybil, 2010), so the concentrations of OC reported from the analyses were used to represent the relative amount of organic matter in each sediment sample.

2.4. *Landscape analysis*

2.4.1. *Catchment-based geological classes and land use types*

A 5 m resolution digital terrain model (DTM; Intermap, 2009) of the study region and hydrological functions in ArcMap9.3^{TM}(ESRI) were used to generate drainage

networks. Upon these were superimposed the locations of each of the 1052 sediment sampling sites and these were snapped to the nearest stream, ensuring that where two streams were close together, the correct stream had been selected by reference to positions which had been recorded on hardcopies of Ordnance Survey maps during sample collection. Hydrological functions and the DTM were used to delineate polygons of the sub-catchment areas draining to each of the sampling sites and the catchment sizes (km^2) were calculated for each.

Digital versions of the 1:50 000 maps of bedrock geology of England – part of DigMap GB of the British Geological Survey (2006)– were used to determine the types and proportions of each bedrock formation which outcrop in each catchment. The catchment polygons were overlaid onto a layer of bedrock polygons with codes for each class in a GIS system; the former were cut into sections using the latter. The GIS was used to calculate the proportions of each bedrock type in each catchment based on the codes for each bedrock formation polygon. Using the same procedure, digital versions of the 25 m resolution Land Cover Map of Great Britain 2000 (Fuller et al., 2002) – with codes for each dominant habitat type – were used to determine their proportions in each catchment of the sediment sampling sites.

To determine the influence of bedrock type on BSP concentration, it was necessary to identify those catchments which were dominated by one lithology and remove any catchments which were anomalously large. Catchments where a single bedrock formation accounted for more than 50% of its area – and where the sub-catchment area was < 55 km^2 – were selected; this left a total of 1052 catchments from 17 geological classes for our analysis. For land use type, the proportions of arable and grassland were determined in each catchment.

2.4.2. *Estimation of mean catchment topsoil P concentration*

To determine average catchment topsoil concentrations, a procedure which combined the proportions of each parent material (PM) – bedrock geology or where present overlying Quaternary deposits – in each catchment with the local concentrations of

total P in topsoil samples was used. This approach is described in greater detail by Appleton et al. (2008). It provides optimal estimates of average catchment topsoil P because the parent material classification accounts for a substantial proportion (33%) of its variation based on an ANOVA analyses undertaken for the current study by the author. In a GIS system, discrete polygons of soil parent material and codes associated with them were created from 1:50 000 scale digital versions of bedrock and Quaternary deposits. Based on location, each topsoil sample P concentration was linked to a unique PM polygon and its associated code. The concentration of topsoil P for each PM polygon was calculated as a distance weighted average for the five nearest samples over the same PM polygon. The catchment boundaries were then overlaid on the parent material polygons to determine the proportion of each unique parent material polygon in each catchment. A final average topsoil P concentration for each catchment was calculated as the area-weighted average of the P concentrations in each of the PM polygons in the catchment.

2.5. *Mid infra red diffuse reflectance spectrometry (MIR-DRS)*

2.5.1. *Diffuse reflectance measurements.*

A Biorad Excalibur series (GS3000MX) fourier transform infra red spectrometer was used for measuring the diffuse reflectance of each sediment sample with a Pike Techologies (Madison, WI) EasiDiff^{TM} accessory. Background spectra were collected using a powdered KBr sample (Pike Technologies, Madison, WI). Each sample was scanned 40 times at a resolution of 4 cm^{-1} in the range 400–4000 cm^{-1}.

2.5.2. *Chemometrics.*

The spectral reflectance data were analysed using the *pls* package (Mevik and Wehrens, 2007) in the R environment (R Development Core Team, 2010) to form partial least squares regression (PLSR) models based on the orthogonal scores algorithm. Cross validation was applied to select the optimum number of components from which to form the PLSR models; prior to forming each model, 10% of the samples were selected

randomly and were not used in model fitting. These samples were then used to assess the model performance by forming predictions and calculating the coefficient of determination (R^2) and root-mean-squared-error of cross validation (RMSE-CV) for between 1 and 12 model components. In the case of Fe_d, the quantity of residual iron in each sample – comprising a range of iron-bearing mineral phases – was calculated as the difference between total Fe (measured by XRFS) and Fe_d.

To determine the significant wavelengths for prediction of the Al_d, Fe_d and OC, both the Variable Importance in the Projection (VIP) (Chong and Jun, 2005) and the PLS regression coefficients (b-coefficients; Haaland and Thomas, 1988) were used. For an observed variable y, the VIP was calculated by:

$$VIP_k(a) \;=\; K \sum_a w_{ak}^2 \left(\frac{SSY_a}{SSY_t} \right) \tag{1}$$

where $\mathrm{VIP}_k(a)$ gives the importance of the kth predictor variable based on a model with a factors, w_{ak} is the corresponding loading weight of the kth variable in the ath PLSR factor, SSY_a is the explained sum of squares of y by a PLSR model with a factors, SSY_t is the total sum of squares of y, and K is the total number of predictor variables. The wavelength is considered important if the values of both the b-coefficients and VIP are sufficiently large. In this study, thresholds for VIP were set to 1 (Chong and Jun, 2005) and the standard deviation of the b-coefficients was applied as their threshold.

The relative quantities of kaolinite and D&M minerals were estimated using specific adsorption features in the MIR spectra. Kaolinite has a sharp, dominant adsorption feature around wavenumber 3700 cm^{-1} (Ferraro, 1982) and D&M minerals around 3625 cm^{-1}. The peak position of these adsorption features varies according to substitution of the mineral lattice (Besson and Drits, 1997) so to estimate their quantities it was decided to use peak area rather than peak height. The area of the D&M peak was between 3600 and 3640 cm^{-1}, whilst the kaolinite peak was between 3683 and 3710 cm^{-1}. Ground reference materials were used to calibrate the kaolinite (Metropolitan Vickers Electrical Co., Manchester, UK) and the D&M (muscovite mica: Hydrite Flat D, Imerys, Georgia, USA) adsorption features. To assess the accuracy of MIR-DRS

for estimating the quantities of kaolinite and D&M minerals in sediment samples, both of these reference materials were added as weighed amounts to a single sediment sample in which both adsorption features were minimal or absent. The addition of the reference materials represented 1, 2, 4, 8, 16 and 20% of the total sample mass on a weight-for-weight basis. Each sample was scanned using the procedure described above and the area under each of the two adsorption features was estimated using a bespoke procedure in the R environment. The percentage quantities of reference material were plotted against the area under the adsorption feature; linear regression models fitted by ordinary least squares to these pairs of points had a coefficient of determination (adjusted R^2) of 0.84 (kaolinite) and 0.81 (D&M) minerals. This was considered sufficient for the purpose of estimating the relative quantities of these two groups of minerals in all sediment samples.

3. Statistical analysis

3.1. *Multiple linear regression*

In this study the following list of ten continuous predictors were selected which could account for variation in BSP concentrations: estimates of BS organic carbon (1), total Fe (2), Fe_d (3), residual Fe (4), Al_d (5), the relative amounts of kaolinite (6) and D&M (7) minerals, total Ce (a REE enriched in P-bearing apatite and P-fertilsers) (8), mineral SSA (9); and average catchment topsoil P concentration (10) . Total Fe was only included for comparison with the other two Fe components (Fe_d and residual Fe) but total Fe was not included in the subsequent multiple regression analysis. The frequency distribution of BSP was strongly positively skewed (skewness coefficient=3.4), so all linear regression analyses were undertaken on log transformed values (skewness coefficient=0.2). As part of an exploratory analysis, simple linear regressoin using ordinary least squares was used to assess the relative importance of these ten predictors and simple scatterplots were created to assess the degree of correlation between them. As might be expected, these plots showed that some predictors were significantly corre-

lated. If these were included in a multiple regression analysis there would be substantial multi-collinearity. To account for this, a principal component analysis was undertaken to elucidate the relationships between a set of orthogonal (uncorrelated) predictors; the scores of the first nine principal components were extracted. To understand how each of the variables relate to each principal component, the eigenvectors were converted to correlation coefficients between the component scores and the original variates using the following equation:

$$c_{ij} \;=\; a_{ij}\sqrt{v_j/\sigma_i^2}\;, \tag{2}$$

where a_{ij} is the ith element of the jth eigenvector, v_j is the jth eigenvalue, and σ_i^2 is the variance of the ith original variable.

These correlations can then be used to examine which variables dominate the variation in each of the principal components. The nine, orthogonal principal components could then be used in a traditional multiple regression analysis – avoiding problems associated with multi-collinearity – based on the interpretation of the variables which dominate the components.

In addition to the nine continuous variables (all excluding total Fe), two other types of predictor were included in the statistical analysis. The first was dominant catchment lithology; which was added to the multiple regression model as a factor with 17 classes. The second was the proportion of arable land and grassland in each of the catchments. These two classes on average accounted for 60% of the land cover in each catchment. Their influence on BSP can be assessed by converting them to compositional variates by taking their additive log ratios (alr; Aitchison, 1986). There are V variables – here the proportions of different land use types within a catchment – which sum approximately to 1 (or 100%). From these are chosen any $V-1$ variables with values for each unit $z_1, z_2, \ldots, z_{V-1}$. These are transformed to:

$$q_i \;=\; \ln\left(\frac{z_i}{z_V}\right) \quad \text{for all } i = 1, 2, \ldots, V-1 \;, \tag{3}$$

where z_V is the value of the remaining Vth variable. The resulting values over all units have by definition a logistic normal distribution, and can be analysed by linear regression – as any other multivariate normal data. So the proportions of land use types (arable or grassland) were converted to their additive log ratios using the reciprocal proportion to close the composition (e.g. 100% minus arable or pasture) and each of the two alr's were included as continuous predictors in the regression analysis.

Multiple regression based on ordinary least squares was preformed with GENSTAT v12.1 (Payne, 2008) using the FIT directive and the ACCUMULATED option. The latter accumulates the analysis of variance and sequentially tests the addition of each predictor to the model to identify whether each predictor is statistically significant. Each of the first 9 principal components (see above) were added to the model, followed by the land use types and the geological classification as a grouped variable. In the regression model, interactions between the geological classification and the nine principal components were also included to test for their significance; where these were statistically significant they were retained.

3.2. *Comparing specific surface area and catchment area*

Previous research has shown that mathematical functions (e.g. power, exponential or linear) can accurately describe relations between river length and features of particle size distributions (psd) (Morris and Williams, 1999 and references therein). In the case of headwater catchments, river (or stream length) can be hard to establish because some may be ephemeral, so in this study, catchment area (section 2.5.1) is used in preference to river length. Given that mineral SSA is strongly related to the psd of sediments and the samples in this study span a range of catchment sizes, it seemed plausible that a mathematical relationship could be established between SSA and catchment size. These two variates were plotted against one another for all 1052 sites and power and

exponential functions were fitted to them using the nonlinear least-squares function (nls) from the MASS library in the R environment (R Development Core Team, 2010). The power function has the form:

$$\mathrm{SSA} = a + b \times \mathrm{A}^c \tag{4}$$

where in this case A is catchment area (km^2) and a, b and c are coefficients.

4. Results and their interpretation

The summary statistics for total BSP concentrations across the study region show that the maximum and minimum concentration varies more than 40-fold (Table 1) reflecting both natural variations in the spatial distribution of native soil P (inherited from parent material), differing rates of fertiliser-P and/or manure application and variations in the efficacy of mechanisms of P delivery to the drainage network. The median fine BSP concentration across the study region (1266 mg kg^{-1}) is consistent with the ranges of values reported for other agricultural catchments in the UK (see Table 6 in Ballantine et al., 2009); however the maximum value (11 480 mg kg^{-1}) is far greater than has been reported elsewhere. Given that the snapshot sampling of BS was undertaken in the summer months, it is likely that the concentration and storage of P is likely to be near its annual maximum (Ballantine et al., 2006).

The mean value of OC measured in 88 samples was 3% (6% organic matter). Direct comparisons with published values for organic carbon in topsoils and subsoils to assess their relative contributions to BS across the region are problematic because of the differences in the size fractions analysed; $<$ 2mm in the case of soil and $<150\mu$m in BS. Total BS iron concentrations were generally large (median 4.9%) reflecting the larger than average concentrations of soil Fe inherited from parent material across this region of England (McGrath and Loveland, 1992).

4.1. *Estimating Fe_d, Al_d and organic carbon by MIR-DRS*

The performance of the PLSR models for the estimation of Fe_d, Al_d and OC by MIR-DRS are summarised in Table 2 and graphically in Figure 3 . For all three variables,

the optimal models consisted of 5 or 6 orthogonal components and in each case the coefficients of determination were large; in the case of model formulation (adj R^2; range 0.8 – 0.89) and for cross-validation (adj R^2; range 0.69 –0.80). The significant adsorption bands (Figure 3) are consistent with published values of specific features in the infra red spectra of organic carbon compounds (Baes and Bloom, 1989), amorphous and crystalline iron oxides (including ferrhydrite, hematite and goethite; Cornell and Schwertmann, 2003) and the OH-stretching region of aluminium oxides (3400 – 3600 cm^{-1}; Elderfield and Hem, 1973).

The cross-validation errors (Table 2) were considered to be sufficiently small to apply the models to estimate the concentrations of each of the three variables in all sediment samples. Summary statistics of the measured and estimated values for each of the three variables (Table 1) show that – with the exception of a few large OC values (cf. Figure 4) – the range of the latter are only slightly larger than the former, although the difference is not sufficient to be of great concern. This might be the case if the PLSR models were extended much beyond the ranges for which they were developed. The median values for the measured and estimated distributions are also quite similar for each of the three variables which suggests that the former are representative of the latter.

4.2. *Simple linear regression*

The results of simple linear regression in which each of the selected predictors (including total Fe and average topsoil P) were used as explanatory variables for the estimation of the log BSP concentration are presented in Table 3. Scatter plots between nine BS properties (including log P concentration) are shown in Figure 5. The BS properties which explain the largest proportion of the variation in log BSP are the concentrations of log Al_d and log Fe_d, these minerals typically have the largest sorption capacities for P in soils (Hartikainen et al., 2010). The concentrations of log Fe_d and log Al_d are strongly correlated (see Figure 4) because they form in similar pedogenic environments and are subsequently transported together. The proportion of variance explained in log

BSP by log Fe_d is substantially larger (27.7%) than either total Fe (20.9%) or residual Fe (16.6%) suggesting that more P is associated with oxyhydroxides of iron than other iron-bearing mineral phases. It is noteworthy from figure 5 that log (total) Fe in BS has strong positive linear correlations with both log Fe_d (Pearson r =0.84) and log Al_d (Pearson $r = 0.76$).

The relative concentration of kaolinite mineral phases account for substantially more of the variation in BSP than D&M minerals; 17.4 and 4.7% respectively. Around twelve percent of BSP was accounted for by the occurrence of organic forms of P which occurs in organic matter. The concentration of the rare-earth element cerium (Ce) also accounts for a substantial portion (10.4%) of the variation in BSP suggesting that a significant quantity of P in BS is associated with REE-enriched apatite or phases derived from the addition of REE-enriched P fertiliser. Mineral SSA did not by itself account for a large proportion of the variance in BSP (1.4%), although it is a statistically significant predictor. Mineral SSA has a strong positive correlation with log Fe_d (Pearson $r = 0.6$) because amorphous forms of the latter commonly account for a large fraction of the surface area of aquatic sediments (Wang et al., 1997). However, as SSA only accounts for a small proportion (0.8%) of the variation in log BSP, BS fractions $>$ around 10μm in diameter must also contain substantial concentrations of P. The scatter plots (Figure 5) demonstrate substantial correlations (linear and log-transformed) amongst some of the bed sediment properties which account for the variation in BSP, specifically kaolinite, Fe_d, Al_d, SSA and Ce. This confirms that it was necessary to undertake multiple linear regression analysis based on the uncorrelated, principal component scores of the significant predictors.

Summary statistics for the proportions of arable and grassland in 547 catchments are shown in Table 4. It is noteworthy that neither of the predictors of the proportions of land use in each catchment (arable or grassland) are statistically significant – they accounted for only small proportions of the variance in BSP (0.1 and 0.45 % respectively). Their influence may be more complex than can be represented by simple

estimates of their proportions in each catchment. For example, more information on the intensity of agricultural inputs, land management practices and connectivity between the hillslopes and channels may be required for the effects of land use type to be fully evaluated.

4.3. *Principal component analysis*

The correlation between the nine variables and their PC scores (Equation **??**) are summarised in Table 5 along with the magnitude of the latent roots and their variances. The first three PCs account for 80% of the variance in the set of nine predictors. The correlations between nine predictors and the first three PC scores are summarised in Figure 6. The first PC is dominated by Fe_d, Al_d and kaolinite. The close association between kaolinite and Fe_d in Figure 6a is particularly strong, although the concentrations of Al_d are also correlated strongly with the other two components. The former can be explained by the stable association between kaolinite and iron oxyhydroxide minerals in pedogenic environments formed by the release of structural iron from the weathering of silicate minerals (Jackson, 1968).

The second and third PCs are dominated by OC and SSA, respectively. Cerium (Ce) has the largest absolute correlation co-efficient with the fourth PC and average catchment topsoil P is the largest in the fifth PC. The largest correlations in component six is for D&M minerals, whist in component seven it is the combination of residual iron and Al_d. Finally, the largest correlations in the eighth and ninth components are for kaolinite and Fe_d. Identification of the dominant features in each of the nine PCs is of importance when interpreting the results of the multiple regression analysis.

4.4. *Multiple linear regression*

Results from the multiple linear regression analysis are presented in Table 6 in the form of an analysis of variance reporting on the addition of predictors to the regression model. The nine sediment-property derived predictors plus the geological classification – and a set of interactions between them – accounted for a large proportion of (61.9%; adjusted R^2) of the variance in log BSP. The first eight of the nine PCs were significant predictors

of BSP ($P < 0.05$) ; the relative importance of each PC can be inferred from their variance ratios (VR) and the increase in adjusted R^2 after addition of each predictor to the model. Larger VRs denote greater predictive power. The most significant predictor (VR=663) is the first PC which was dominated by Fe_d, Al_d and kaolinite; much BSP is sorbed to the surfaces of iron and aluminium oxyhydroxides and these phases appear to be strongly associated with kaolinite.

Both PC five (VR=281) and PC four (VR=270) are of similar predictive power. The fourth PC was most strongly correlated with Ce – indicative of primary P-bearing apatite or REE enriched P-fertiliser phases – suggesting that these make a significant contribution to BSP. The fifth PC was dominated by average catchment topsoil P indicating that – as might be expected – its variations between catchments has a substantial impact on BSP content. Organic matter dominated PC 2 which is the next most significant predictor (VR 156) and denotes the occurrence of organic forms of P in BS. Component 7 also has a large VR (121) which appears to be related to residual iron phases and non-crystalline aluminium. Scanning electron microscopy with energy-dispersive X-ray microanalysis of selected BS samples (not shown) confirmed that Fe-phosphate phases were present in some cases. The remaining PCs (3,6 and 8) have relatively modest VRs (range 7 – 52) by comparison with those reported above. The third PC, which was dominated by mineral SSA, has a relatively small VR (15.2) confirming that its role in influencing BSP is relatively minor.

A non-paired, two-sided t-test showed there was no statistically significant difference at the 5% confidence level (P=0.058) between total topsoil P at arable (n=4310) and grassland (n=1836) sites across the region based on the dominant land use recorded at the soil sampling location. However, the inclusion of the proportions of arable and grassland in each catchment showed that these were both significant predictors with relatively small VRs (8 and 9). The model co-efficients are negative for arable (-0.004) and positive (0.008) for grassland; this may be attributable to the transportation of larger particle size fractions – which contain smaller quantities of P – from arable

catchments, thus diluting BSP.

The geological classification was also a significant predictor (VR 6.4); it accounts in part for the processes controlling the transport and delivery of P to BS. The significance of the interactions between the 17 geological classes and the other PC-based explanatory variables were also tested by adding them to the regression model; four were found to be significant (PCs 1, 2, 3, and 7) although the VRs are modest (range 2.2–2.4). Stronger interpretations can be placed on the first three PCs because their scores had larger correlation coefficients with specific sediment properties (see Table 4). So the regression model includes 17 coefficients for geological class relating to each of the following: PC1 (Fe_d, Al_d and kaolinite content), PC2 (organic carbon content), PC3 (specific surface area) and PC7 (residual iron and log Al_d).

4.5. *Specific surface area versus catchment area*

A scatter plot of catchment area versus BS mineral SSA based on the measured values (n=56) and estimates from geochemistry (Rawlins et al., 2010) are shown in Figure 7. The power function provided the best fit between catchment area and BS mineral SSA. The values of the model coefficients a, b and c (Equation **??**) and the standard errors (in parenthesis) were: −32.0 (7.6), 15.9 (4.9) and 0.40 (0.05), respectively. The fitted model had a residual standard error of 3.2 and accounted for 86% of the variance in mineral SSA (un-adjusted R^2=0.86). In a previous study, Rawlins et al. (2010) had shown that dominant catchment bedrock type accounted for 39% of the variance in estimates of mineral SSA from the same region, albeit from a somewhat larger dataset (n=1236). Catchment size – or channel length – is clearly the dominant factor determining BS SSA (Figure 7) and the significance of bedrock type highlighted by Rawlins et al. (2010) was due to the influence of dominant lithology on geomorphology and hydrogeology which forms catchments with constrained size ranges. Although the well-established phenomenon of downstream fining based on particle size (Morris and Williams, 1999) has not previously been extended to encompass mineral SSA, it most likely accounts for the relationship between mineral SSA and catchment size shown in

Figure 7. Considering that the location of BS sampling sites were not selected on the basis of local stream flow regime (i.e. sampling was not biased towards pools or riffles), the relationship between catchment size and fine BS SSA is remarkably consistent.

5. Discussion

The focus of this study was to determine the controls on BSP concentrations at the landscape-scale using a range of quantitative sediment properties and catchment characteristics to aid the understanding of processes relating to PP loss from catchments. A widely-used, process-based model of phosphorus (P) and sediment mobilisation (PSYCHIC; Davison et al., 2007) has a range of spatial input data including information on crops, P application rates, soil properties (including texture, organic carbon and bulk density), climate data, slope and population density. In PSYCHIC, the finer fractions of eroded soil are enriched in P (ratios 0.1 sand: 0.25 silt: 1 clay), but the model does not account for the spatial distributions of Al and Fe oxyhydroxides which, as shown in this study and previously (House et al., 1995), are the dominant phases with which P is associated in BS across areas dominated by silicate bedrock.

Statistical analysis showed that both log Fe_d and Al_d were strongly correlated with total log Fe in BS, so the latter could be used to estimate the former. In addition, there is a positive relationship between topsoil Fe concentrations and BSP across the 1052 catchments (Pearson linear correlation r=0.23); a least squares regression model shows that this relationship is statistically significant, accounting for 5.2% of the variance in BSP. Geochemical survey data coupled with high-resolution maps of soil parent material across England and Wales can now provide accurate estimates of major element concentrations such as Fe in soil at scales finer than 1 km^2 (Appleton et al., 2008). The spatial distribution of soil Fe – with a coefficient for P enrichment – might effectively be incorporated into process-based models such as PSYCHIC to improve estimates of PP transfer to BS in agricultural catchments in areas dominated by silicate bedrock. In regions of carbonate bedrock – such as the Cretaceous chalk dominated catchments of southern and eastern England – the importance of carbonate

phases in controlling forms of BSP may, in part, negate the role of iron oxyhydroxides and non-crystalline aluminium phases. The spatial distribution of soil and BS Fe could also aid understanding of where ecological risks associated with large concentrations of bioavailable-P are likely to be mitigated by adsorption on the surfaces of Al and Fe oxyhydroxides (Palmer-Felgate et al., 2009).

The importance of field drains as a pathway for rapid transfer of PP to stream channels was not included in this study because accurate information on the distribution and functioning of drains was not available at a sufficiently fine spatial resolution (Chapman et al., 2003). For the same reason, information on point source inputs of phosphorus from sewage treatment works, septic tanks or agricultural point sources such as farmyards were not incorporated into the analysis. No attempt was made to investigate the connectivity of hydrological flow pathways from critical sources areas and its impact on mobilisation and delivery of PP to catchment channels (Heathwaite et al., 2005). Such approaches typically require high-resolution (lidar) topographic data which is not available across all our study area. In subsequent analysis, models of sediment mobilisation and delivery could be applied to a subset of the studied catchments to investigate the significance of hydrological connectivity. Catchments could be selected to maximise both the variation in hydrological connectivity from potential contributing source areas and also the components which dominate BSP: i) kaolinite and oxyhydroxides of Al and Fe, ii) organic matter and, iii) the rare earth signatures of naturally occurring apatite or P-fertiliser/manure inputs.

Landscape-scale variation in bedrock geology was shown to be significant factor controlling BSP concentrations based on statistical analysis. The approach of using of a single, dominant bedrock class for each catchment in the model could be improved in subsequent analysis. First, by accounting for the proportions of the different bedrock types in each catchment and linking them to critical source areas. Second, by using parent material distributions at 1:50 000 scale (i.e. including Quaternary deposits) rather than just bedrock types across the catchments. In recently glaciated landscapes such

as those in central England, soil parent material class explains more of the variation of soil properties than simple bedrock lithology (Rawlins et al., 2003).

Organic matter content had a significant positive correlation with BSP at the landscape-scale; although this relationship has been reported previously (Ballantine et al., 2009) it is not observed consistently (Palmer-Felgate et al., 2009). Where possible, the snapshot sampling protocol adopted by the G-BASE project collects BS from active parts of channels, avoiding areas with low flow velocities where sedimentation of fine organic debris may be enhanced. It is therefore unlikely that this could lead to a positive sampling bias in the reported median organic carbon values (3%; or 6% organic matter) across the study region.

Fingerprinting of P in BS of agricultural catchments – either from apatite or REE-enriched P-fertiliser based on their Ce content – has not, to the authors knowledge been demonstrated previously. Quantifying the relative importance of these two P sources (native P or fertiliser/manure-derived P) for BSP would be a considerable research challenge. One potential means of assessing their relative contributions would be to measure the REE profiles of sediment collected from soil erosion experiments in which applied P and native P have markedly different REE fractionation. However, other soil minerals would also contribute to the REE signature of runoff sediment and this may limit the scope for discriminating between the native and applied-P derived REE signatures.

Both organic and a range of inorganic mineral components in fine BS were estimated accurately using MIR-DRS based on unique adsorption features and using chemometric approaches across the full mid-IR spectrum. As shown, BSP is closely associated with these phases, so MIR-DRS – which when used with non-absorbing, powdered KBr requires less than 0.1 g of sample – could be used to monitor changes in their concentrations in suspended sediment samples through storm events to elucidate PP dynamics. Based on measurements of total nitrogen (not reported) from the same subset of 88 BS samples for which OC was determined, it was also possible to accu-

rately estimate the former (adj R^2 0.79; RMSE-CV=0.06%) across a range of total N from 0.1% to 0.51%. Landscape-scale data on the concentrations of total OC, N and P in BS could enhance our understanding of nutrient cycling and losses from agricultural systems (Quinton et al., 2010). Establishing the relative quantities of particulate OC and mineral-stabilised OC in fine bed sediments using MIR-DRS (Zimmerman et al., 2007) could also aid fingerprinting of inputs from topsoil and subsoil landscape compartments (e.g. Fontaine et al., 2007).

To the authors knowledge, the very strong relationship reported between fine (<150μm) BS mineral SSA and catchment area (range 5-55 km^2) has not been observed before. Bedrock in this region largely comprises a range of silicate-dominated sedimentary sequences. Further investigation is required to assess the nature of this relationship in larger catchments and whether it differs significantly in landscapes with other bedrock types and geomorphic settings.

6. Conclusions

The main conclusions from this study are:

1. MIR-DRS is a cost-effective and rapid means to quantify the organic and mineral composition of BS samples. Accurate estimates were made of five components (Al_d, Fe_d, OC, kaolinite and D&M minerals) in 1052 BS from individual agricultural headwater catchments.

2. Simple linear regression demonstrated that the proportion of variance in BSP explained by specific components across all catchments declined in the following order: Al_d > Fe_d > topsoil P = kaolinite = residual iron > organic matter = Ce > D&M > mineral SSA. There was significant correlation amongst these individual predictors of BSP so their scores on nine PCs were used in a multiple regression analysis to elucidate relationships with BS more clearly.

3. The multiple regression model accounted for 61.9% of the variance in BSP. The first PC which was dominated by Al_d, Fe_d and kaolinite was the most important

predictor, but organic matter and average catchment topsoil P also accounted for large proportions of the variance. There was a very strong positive linear correlation between the relative quantity of kaolinite and Fe_d in BS which is related to their contemporaneous formation and association in pedogenic environments and subsequent joint transport to BS.

4. Cerium (Ce) content of BS is the dominant feature of one of the PCs and accounts for a substantial proportion of the variation in BSP; it was inferred that Ce denotes some combination of input from either REE-enriched native P or fertilser/manure-P, but the relative importance of these two sources cannot be assessed based on the available data.

5. A classification based on dominant bedrock geology in each catchment – and four interactions with other BS predictors – was statistically significant because bedrock type partly accounts for the processes controlling the transport and delivery of PP to headwater BS.

6. The proportions of arable and grassland by area in each catchment explained a small, statistically significant proportion of the variation in BSP in the MRM.

7. Mineral SSA – estimated using four BS geochemical predictors – explained only a small proportion of the variation in BSP. A power function fitted between estimates of mineral SSA and catchment area (range 5-55 km^2) explained 86% of the variation in the former. This is largely due to the well-established phenomenon of downstream fining, but this has not hitherto been extended to encompass mineral SSA.

8. There was a positive relationship between topsoil Fe and BSP. Process-based models of PP mobilisation – which do not currently account for the spatial distribution of soil Fe – might be improved by including estimates of topsoil Fe with a coefficient for P enrichment using high-resolution maps of soil parent material

and geochemical survey data. Incorporating data on the distribution of soil Fe into models of P mobilisation could enhance estimates of P delivery to BS.

Acknowledgements

This paper is published with the permission of the Executive Director of the British Geological Survey (Natural Environment Research Council). The Land Cover information in England was provided under licence by the Centre for Ecology and Hydrology (©NERC 2008). I acknowledge the contributions of all staff from the British Geological Survey involved in the bed sediment and soil survey of central England: (i) the G-BASE project staff who organized the collection and processing of the stream sediment data, (ii) the staff who prepared the samples, and (iii) the analytical staff who did the XRF-S analysis (iv) and the MIR scanning of the sediment samples. I would also like to thank Murray Lark for some advice regarding the statistical analysis and Don Appleton for assistance with the estimation of topsoil P. I would like to thank an anonymous reviewer for comments which improved the manuscript.

References

Abdel-Haleem, A.S., Sroor, A., El-Bahi, S. M., Zohny, E. 2001. Heavy metals and rare earth elements in phosphate fertilizer components using instrumental neutron activation analysis. Appl. Radiat. Isotopes. 55, 569–573.

Aitchison, J. 1986. *The Statistical Analysis of Compositional Data.* Chapman & Hall, London.

Appleton, J.D., Rawlins, B.G., Thornton, I. 2008. National-scale estimation of potentially harmful element ambient background concentrations in topsoil using parent material classified soil:streamsediment relationships. Appl. Geochem. 23, 2596–2611.

Baes, A.U., Bloom, P.R., 1989. Diffuse reflectance and transmission Fourier-transform infrared (Drift) spectroscopy of humic- and fulvic acids. Soil Sci. Soc. Am. Proc. 53, 695–700.

Ballantine, D., Walling, D., Collins, A. & Leeks, G. 2006. Phosphorus Storage in Fine Channel Bed Sediments. Water Air Soil Poll. - Focus. 6, 371–380.

Ballantine, D. J., Walling, D. E., Collins, A. L. & Leeks, G. J. L. 2009. The content and storage of phosphorus in fine-grained channel bed sediment in contrasting lowland agricultural catchments in the UK. Geoderma. 151, 141–149.

Bera, R., Seal, A., Banerjee, M., Dolui, A. K. 2005. Nature and profile distribution of iron and aluminum in relation to pedogenic processes in some soils developed under tropical environment in India. Environ. Geol. 47, 241–245.

Bertaux, J., Froehlich, F., Ildefonse, P. 1998. Multicomponent analysis of FTIR spectra: quantification of amorphous and crystallized mineral phases in synthetic and natural sediments. J. Sediment. Res. 68, 440–447.

Besson, G., Drits, V. A. 1997. Refined relationships between chemical composition of dioctahedral fine-grained micaceous minerals and their infrared spectra within the OH stretching region .2. The main factors affecting OH vibrations and quantitative analysis. Clay. Clay Miner. 45, 170–183

Beven, K., Heathwaite, L., Haygarth, P., Walling, D., Brazier, R. & Withers, P. 2005. On the concept of delivery of sediment and nutrients to stream channels. Hyd. Proc. 19, 551–556.

British Geological Survey 2006. *Digital Geological Map of Great Britain 1:50 000 scale (DiGMapGB-50) data [CD-ROM] Version 3.14*. British Geological Survey, Keyworth, Nottingham.

Chapman, A. S., Foster, I. D. L., Lees, J. A., Hodgkinson, R. J., Jackson, R. H. 2003. Sediment and phosphorus delivery from field to river via land drains in

England and Wales. A risk assessment using field and national databases. Soil Use Manage. 19, 347–355.

Chong, I.-G., Jun, C.-H., 2005. Performance of some variable selection methods when multicollinearity is present. Chemometr. Intell. Lab. 78, 103–112.

Cornell, R. M., Schwertmann, U. 2003. *The Iron Oxides: Structure, Properties, Reactions, Occurrences and Uses: Chapter 3 – Characterization.* WILEY-VCH, Weinheim, p 139–183.

Davison, P., Withers, P. J. A., Lord, E. I., Betson, M. J. and Stromqvist, J. 2007. PSYCHIC - a process based model of phosphorus and sediment mobilisation and delivery within agricultural catchments. Part 1: Model description and parameterisation. J. Hydrol. 350, 290–302.

Edzwald, J. K., Toensing, D. C., Leung, M. C.-Y. 1976. Phosphate adsorption reactions with clay minerals. Env. Sci. Technol. 10, 485–490.

Elderfierld, H., Hem, J. D. 1973. The development of crystalline structure in aluminium hydroxide polymorphs on ageing. Mineral. Mag. 39, 89–96.

Emerson SM, Widmer G. 1978. Early diagenesis in anaerobic lake sediments II: Thermodynamic and kinetic factors controlling the formation of iron phosphate. Geochim. Cosmochim. Ac. 42, 1307–1316.

Evans, D.J., Johnes, P.J., Lawrence, D.S. 2004. Phsico-chemical controls on phosphorus cycling in two lowland streams. Part 2-The sediment phase. Sci. Tot. Env. 329, 165–182.

Ferraro, J. R. 1982. The Sadtler infrared spectra handbook of minerals and clays. Heyden & Son Ltd. London. 440 pp.

Fontaine, S., Barot, S., Barre, P., Bdioui, N., Mary, B., Rumpel, C. 2007. Stability of organic carbon in deep soil layers controlled by fresh carbon supply. Nature.

450, 277–280.

Fuller, R.M., Smith, G. M., Sanderson, J. M., Hill, R.A., Thomson, A.G. 2002. The UK Land Cover Map 2000: Construction of a parcel-based vector Map from satellite images. Cartogr. J. 39,15–25

Haaland, D.M., Thomas, E.V., 1988. Partial least-squares methods for spectral analyses.1. Relation to other quantitative calibration methods and the extraction of qualitative information. Anal. Chem. 60, 1193–1202.

Hartikainen, H., Rasa, K., Withers, P.J.A. 2010. Phosphorus exchange properties of European soils and sediments derived from them. Eur. J. Soil Sci. DOI: 10.1111/j.1365-2389.2010.01295.x

Heathwaite, A.L., Quinn,P.F., Hewett, C. J. M. 2005. Modelling and managing Critical Source Areas of diffuse pollution from agricultural land using flow connectivity simulation. J. Hydrol. 304, 446–461

House W.A., Denison F.H., Armitage P.D. 1995. Comparison of the uptake of inorganic phosphorus to a suspended and streambed sediment. Water Res. 29, 767–779.

House, W. A. 2003. Geochemical cycling of phosphorus in rivers. Appl. Geochem. 18, 739–748.

Intermap, 2009. NEXTMap Britain. Intermap. http://www.intermap.com/nextmapbritain. Accessed 6.12.09).

Jackson, M.L. 1968. Weathering of primary and secondary minerals in soils. Trans. Int. Congr. Soil Sci. 4, 281–282.

Johnson, C. C., Breward, N., Ander, E. L., Ault, L. 2005. G-BASE: Baseline geochemical mapping of Great Britain and Northern Ireland. Geochem. Explor. Environ. Anal. 5, 1–13.

Koschel, R., Benndorf, J., Proft. G., Rechnagel, F. 1978. Calcite precipitation as a natural control mechanism of eutrophication. Arch. Hydrobiol. 98, 380–408.

Madari, B. E., Reeves III, J. B., Machado, P. L. O. A., Guimares, C. M., Torres, E., McCarty, G. W. 2006. Mid- and near-infrared spectroscopic assessment of soil compositional parameters and structural indices in two Ferralsols. Geoderma. 136, 245–259.

Martinez-Carreras, N., Krein, A., Udelhoven, T., Gallart, F., Iffly, J., Hoffmann, L., Pfister, L., Walling, D. 2010. A rapid spectral-reflectance-based fingerprinting approach for documenting suspended sediment sources during storm runoff events. J. Soils Sediments. 10, 400–413.

McGrath, S. P., Loveland, P. J. 1992. *The Soil Geochemical Atlas of England and Wales*, Blackie Academic and Professional, Glasgow.

Mevik, B.H. and Wehrens, R., 2007. The pls Package: Principal Component and Partial Least Squares Regression in R. J. Stat. Soft. 18, 1–24.

Morris, P.H. and Williams, D.J. 1999. A worldwide correlation for exponential bed particle size variation in subaerial aqueous flows. Earth Surf. Proc. Land. 24, 835–847.

Palmer-Felgate, E.J., Jarvie, H.P., Withers, P.J.A., Mortimer, R.J.G., Krom, M.D. 2009. Stream-bed phosphorus in paired catchments with different agricultural land use intensity. Agr. Ecosyst. Environ. 134, 53-66.

Payne, R.W. (ed) 2008. *GenStat Release 11 Reference Manual. Part 2 Directives.* VSN International, Hemel Hempstead.

Plant, J. A. 1971. Orientation studies on stream sediment sampling for a regional geochemical survey in northern Scotland. T I MIN METALL B, 234–345.

Prybil, D. W. 2010. A critical review of the conventional SOC to SOM conversion factor. Geoderma. 156, 75–83.

Quinton, J.N., Govers, G., Van Oost, K., Bardgett, R.D. 2010. The impact of agricultural soil erosion on biogeochemical cycling. Nature Geosci. 3, 311–314.

R Development Core Team, 2010. R: A Language and Environment for Statistical Computing., R Foundation for Statistical Computing, Vienna, Austria, http://www.R-project.org.

Rawlins, B. G., Turner, G., Mounteney, I. & Wildman, G. 2010. Estimating specific surface area of fine stream bed sediments from geochemistry. Appl. Geochem. 25, 1291–1300

Rawlins, B.G., Webster, R., Lister, T.R. 2003. The influence of parent material on top soil geochemistry in eastern England. Earth Surf. Proc. Land. 28, 1389–1409.

Smith, V. H. 2003. Eutrophication of freshwater and coastal marine ecosystems: a global problem. Environ. Sci. Pollut. Res. Int. 10, 126–139.

Soil Survey of England and Wales, 1983a. *Soils and their Use in Midland and Western England.* Ordnance Survey for the Soil Survey of England and Wales, Southampton.

Soil Survey of England and Wales, 1983b. *Soils and their Use in Eastern England.* Ordnance Survey for the Soil Survey of England and Wales, Southampton.

Starinsky, A., Katz, A., Kolodny, Y. 1982. The incorporation of uranium into diagenetic phosphorite. Geochim. Cosmochim. Ac. 46, 1365–1374.

Sylvester-Bradley, P.C. and Ford, T.D. 1968. *The geology of the East Midlands.* Leicester University Press, 400pp.

van der Perk, M., Owens, P. N., Deeks, L. K., Rawlins, B. G., Haygarth, P. M., Beven, K. J. 2007. Controls on catchment-scale patterns of phosphorus in soil, streambed sediment, and stream water. J. Environ. Qual. 36, 694–708.

van der Perk, M., P.N. Owens, L.K. Deeks, and B.G. Rawlins. 2006. Sediment geochemical controls on in-stream phosphorus concentrations during base flow. Water Air Soil Poll. 6, 443–451.

Wang, F., Chen, J., Chen, J., Forsling, W. 1997. Surface properties of natural aquatic sediments. Wat. Res. 31, 1796–1800.

Withers, P.J.A., Edwards, A.C., Foy, R.H., 2001. Phosphorus cycling in UK agriculture and implications for phosphorus loss from soil. Soil Use Manage. 17, 139–149.

Zimmermann, M., Leifeld, J., Fuhrer, J. 2007. Quantifying soil organic carbon fractions by infrared-spectroscopy. Soil Biol. Biochem. 39, 224-231.

Figure captions

Fig.1 Simplified geological map of the study region.

Fig.2 Map of the study region showing topography, urban areas and major rivers.

Fig.3 Wavelengths for which both variable importance in the projection (VIP) scores and regression (beta) coefficients are significant (see text) in partial least squares models of reflectance spectra for prediction of: a) Al_d, b) Fe_d and c) organic carbon (OC).

Fig.4. Measured and predicted values for selected bed sediments: a) Al_d (mg kg^{-1}; n=60), b) Fe_d (mg kg^{-1}; n=60), b) total organic carbon (%; n=88) based on mid infra red diffuse reflectance spectrometry.

Fig.5. Matrix of scatterplots for properties of fine bed sediments (n=1052) from headwater catchments and catchment area: log P=log phosphorus concentration (mg kg $^{-1}$), cerium (Ce;mg kg $^{-1}$), OC = organic carbon (%), D&M minerals (relative scale), kaolinite (relative scale), log Fe(d; mg kg $^{-1}$), log Al(d; mg kg^{-1}), SSA=specific surface area (m^2 g^{-1}), catch. area = catchment area (km^2).

Fig.6 Projections of the correlations between variables and the principal component scores in unit circles: a) component 2 against component 1; b) component 3 against component 1. Variable notation: SSA=specific surface area, OC=organic carbon, k=kaolinite, D&M=dioctahedral clay and mica, Fe_d =dithionite extractable iron , Al_d =dithionite extractable aluminium , soil P= mean catchment topsoil phosphorus, res Fe=residual iron.

Fig.7 Fine bed sediment mineral specific surface area versus catchment area (km^2) at 1052 sampling sites. The dashed line is a power function fitted to the data (see text).

Table 1 Selected statistics for measured and MIR-DRS estimated properties of fine bed sediments and topsoil across the study region. Element concentrations in mg kg $^{-1}$.

	Sediments										Topsoil
	*OC (%)		Fe_d		Al_d		†SSA		Fe	P	**P
	meas.	est.	meas.	est.	meas.	est.	meas.	est.	meas.	meas.	meas.
Min.	0.5	0.2	4974	4585	265	249	5.98	1.60	16020	262	87.2
Max.	6.0	9.7	90140	105700	4747	5430	50.5	63.3	213000	11480	11826
Median	2.9	3.2	18940	22580	1114	944	20.1	23.2	49450	1266	829
Mean	3.0	3.2	20410	23440	1192	1045	22.7	23.7	52910	1447	1008
St. Dev.	1.2	1.1	13041	12512	690	538	10.1	8.61	19670	763	584
Skewness	0.32	0.34	2.63	1.23	2.6	2.3	0.54	0.37	1.54	3.43	3.93
Counts	88	987	60	1015	60	1015	56	1015	1052	1052	7233

* Organic Carbon

** <2 mm size fraction

†units g m^{-2}

meas.=measured,est.=estimated

Table 2 Selected features of optimal partial least squares regression models for estimation of Al_d, Fe_d and organic carbon in bed sediments.

Property	[a] n components	adj R^2	adj R^2-CV	[b] RMSEP-CV
[c]Al_d	5	0.80	0.69	0.29
[c]Fe_d	5	0.89	0.80	0.25
Org. Car.	6	0.88	0.80	0.53

[a] number of orthogonal PLSR components

[b] cross validation adjusted R^2

[c] root mean square error of cross validation (RMSEP-CV) given in log units

Table 3 Summary statistics from simple linear regression by ordinary least squares for log bed sediment P (n=1052) for a range of explanatory variables.

Predictor	Estimate	Std. Error	P-value	adjusted R^2 (%)
log Al_d	0.583	0.024	<0.001	35.6
log Fe_d	0.44	0.021	<0.001	28.4
log Fe	0.62	0.035	<0.001	23.0
[a]residual Fe	-0.59	0.04	<0.001	16.4
kaolinite	241	16.1	<0.001	17.4
[b]topsoil P	0.53	0.035	<0.001	18.2
Organic carbon	0.135	0.01	<0.001	11.6
Ce	0.008	69.4×10^{-5}	<0.001	10.4
[c] D&M	-1.07	0.146	<0.001	4.7
SSA	0.006	0.001	<0.001	1.4
[d] Arable	-0.008	0.006	0.163	0.1
[d] Grassland	0.004	0.004	0.333	0.45

[a]residual Fe is total Fe_d minus total Fe determined by XRFS (see text)

[b] average catchment topsoil P

[c] dioctahedral clay and mica minerals

[d] log ratios of the proportions of land use type:all other land use types

Table 4 Summary statistics for the proportions of permanent grassland and arable land in a subset of 547 catchments in which the sum of their proportions accounts for more than 70% of the total catchment area. All proportions as percentages (%).

Statistic	Arable	Permanent grassland
Min	0.1	0.1
Median	35	24
Mean	38.9	22.7
Max	99.9	99.9
St. Dev.	23.8	21.8

Table 5 Correlations between variables and their principal component scores for nine selected predictors. The latent roots and accumulated variance (%) are also reported. Selected large positive and negative coefficients in **bold**.

	Principal Component								
	1	2	3	4	5	6	7	8	9
SSA	0.64	0.04	**0.58**	0.41	0.27	−0.04	−0.11	0.006	0.028
OC	0.05	**-0.94**	0.23	−0.15	−0.04	0.21	−0.01	−0.03	−0.02
Fe_d	**0.96**	-0.04	0.02	−0.07	0.04	−0.16	0.06	0.07	**−0.19**
[a]resid Fe	**−0.82**	0.22	0.35	0.17	−0.13	0.17	**0.28**	0.08	0.04
Soil P	0.73	0.08	0.05	0.22	**0.63**	0.04	−0.11	0.01	0.002
D&M	0.82	0.16	−0.29	0.22	0.16	**0.29**	0.09	−0.18	0.03
kaolinite	**0.91**	−0.06	−0.22	0.02	0.07	0.16	0.05	**0.28**	0.07
Al_d	**0.89**	-0.17	0.11	−0.11	−0.07	−0.22	**0.27**	−0.09	0.10
Ce	0.56	0.47	0.34	**−0.56**	0.002	0.17	−0.06	− 0.02	0.01
Latent roots	5.18	1.22	0.77	0.65	0.53	0.29	0.19	0.13	0.05
acc. Var. (%)	57.5	71.0	79.5	86.7	92.6	95.8	97.9	99.4	100

[a] total Fe_d minus the total concentration of iron determined by XRFS (see text)

acc. Var. = accumulated variance

Table 6 Analysis of variance summary following sequential inclusion of eight principal component predictors (Comp), the proportion of land use types and a dominant catchment geological classification (Geol) in a multiple linear regression model to predict log bed sediment P concentrations. Specific interactions (*) between the principal components and the geological classification are also listed.

Predictor	Deg. freedom	Sum squares	Mean square	Var. ratio	*P*-value	adjusted R^2 (%)
Comp 1	1	50.8	50.8	663	<.001	24.1
Comp 2	1	11.9	11.9	156	<.001	29.7
Comp 3	1	1.17	1.17	15.2	<.001	30.2
Comp 4	1	20.7	20.7	270	<.001	39.9
Comp 5	1	21.5	21.5	281	<.001	50.2
Comp 6	1	0.499	0.499	6.52	0.011	50.3
Comp 7	1	9.23	9.23	121	<.001	54.7
Comp 8	1	3.96	3.96	51.8	<.001	56.6
Arable	1	0.688	0.688	8.99	0.003	56.9
Pasture	1	0.606	0.606	7.91	0.005	57.1
Geol	17	4.54	0.267	3.49	<.001	58.6
Comp 1*Geol	17	3.00	0.177	2.31	0.002	59.4
Comp 2*Geol	17	2.81	0.165	2.16	0.004	60.1
Comp 3*Geol	17	2.78	0.173	2.27	0.002	60.9
Comp 7*Geol	17	2.92	0.183	2.39	0.002	61.9
Residual	956	73.36	0.077			
Total	1051	210	0.200			

Figure 1:

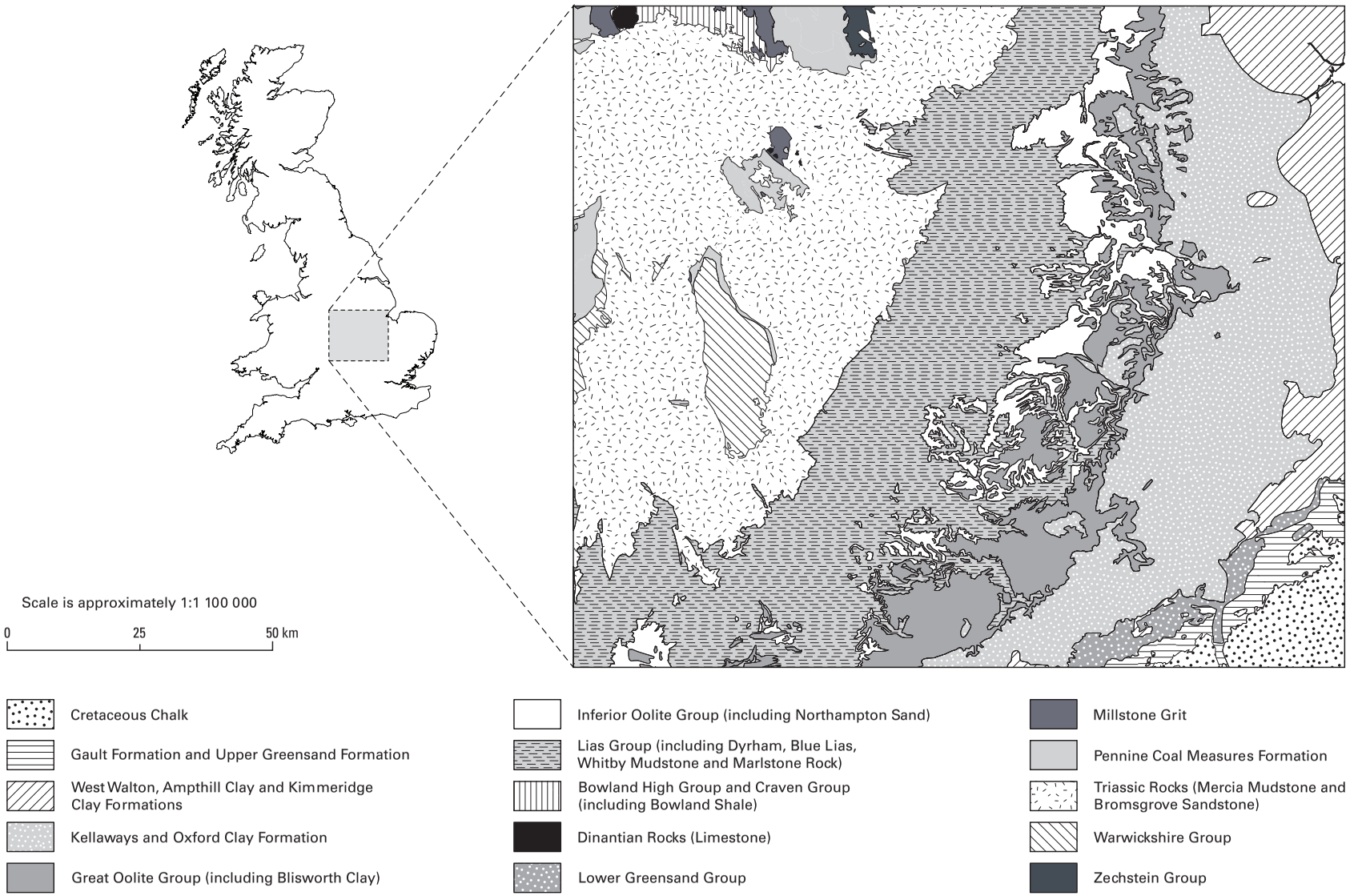
Scale is approximately 1:1 100 000
0
25
50 km
Cretaceous Chalk
Gault Formation and Upper Greensand Formation
West Walton, Ampthill Clay and Kimmeridge Clay Formations
Kellaways and Oxford Clay Formation
Great Oolite Group (including Blisworth Clay)
Inferior Oolite Group (including Northampton Sand)
Lias Group (including Dyrham, Blue Lias, Whitby Mudstone and Marlstone Rock)
Bowland High Group and Craven Group (including Bowland Shale)
Dinantian Rocks (Limestone)
Lower Greensand Group
Millstone Grit
Pennine Coal Measures Formation
Triassic Rocks (Mercia Mudstone and Bromsgrove Sandstone)
Warwickshire Group
Zechstein Group

Figure 2:

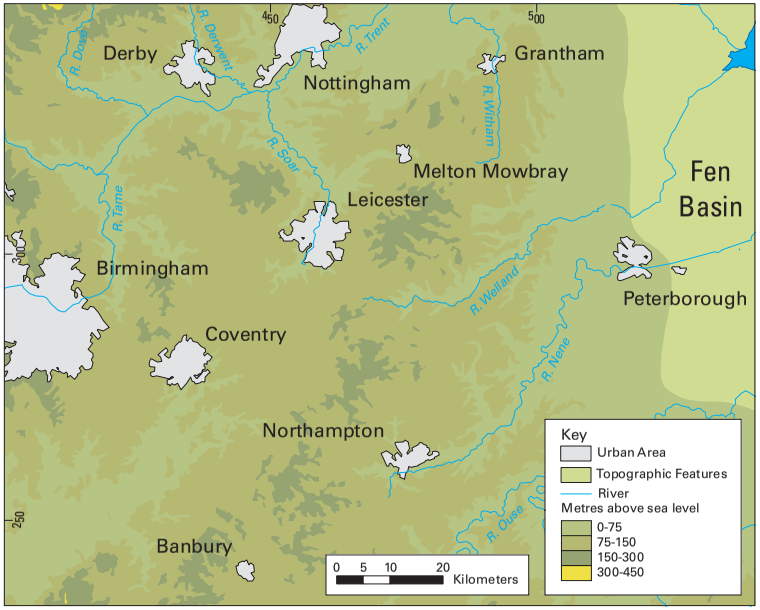
Derby
Nottingham
Grantham
Melton Mowbray
Leicester
Birmingham
Coventry
Northampton
Banbury
Peterborough
Fen Basin
R. Dove
R. Derwent
R. Trent
R. Witham
R. Soar
R. Tame
R. Welland
R. Nene
R. Ouse
450
500
300
250
Key
Urban Area
Topographic Features
River
Metres above sea level
0-75
75-150
150-300
300-450
0 5 10 20
Kilometers

Figure 3:

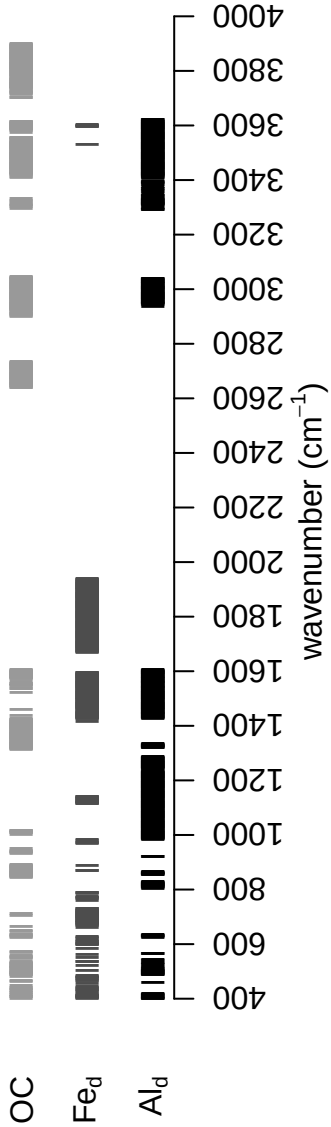
OC
Fe$_d$
Al$_d$
400
600
800
1000
1200
1400
1600
1800
2000
2200
2400
2600
2800
3000
3200
3400
3600
3800
4000
wavenumber (cm^{-1})

Figure 4:

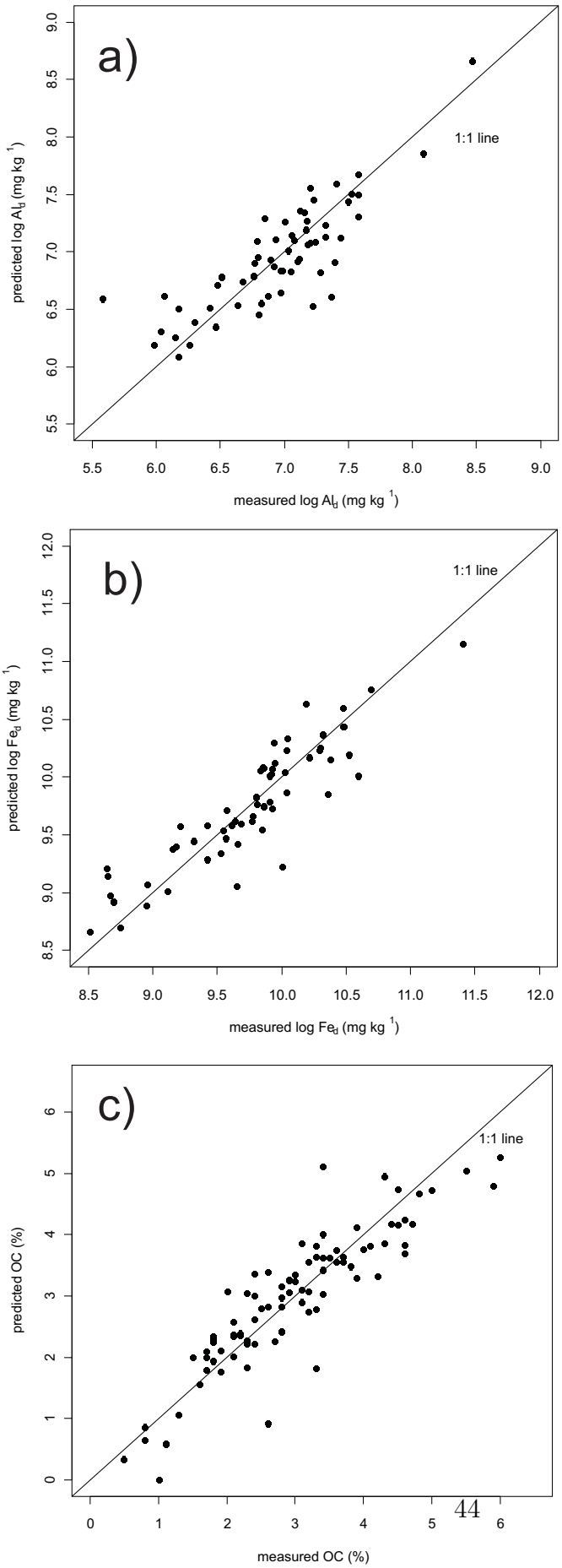
a)
1:1 line
predicted log Al$_d$ (mg kg^{-1})
measured log Al$_d$ (mg kg^{-1})
5.5
6.0
6.5
7.0
7.5
8.0
8.5
9.0
b)
1:1 line
predicted log Fe$_d$ (mg kg^{-1})
measured log Fe$_d$ (mg kg^{-1})
8.5
9.0
9.5
10.0
10.5
11.0
11.5
12.0
c)
1:1 line
predicted OC (%)
measured OC (%)
0
1
2
3
4
5
6

Figure 5:

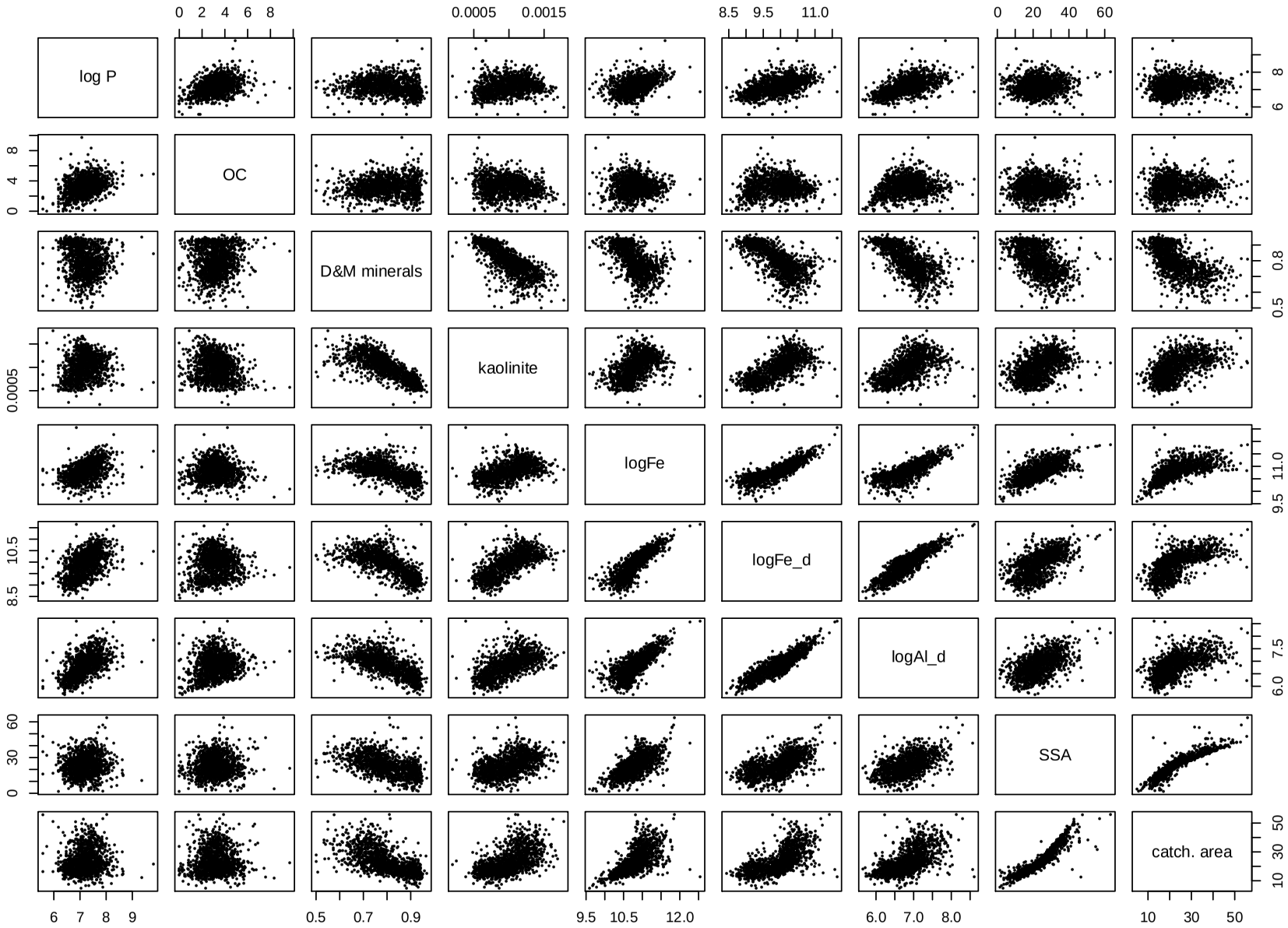
log P
OC
D&M minerals
kaolinite
logFe
logFe_d
logAl_d
SSA
catch. area

Figure 6:

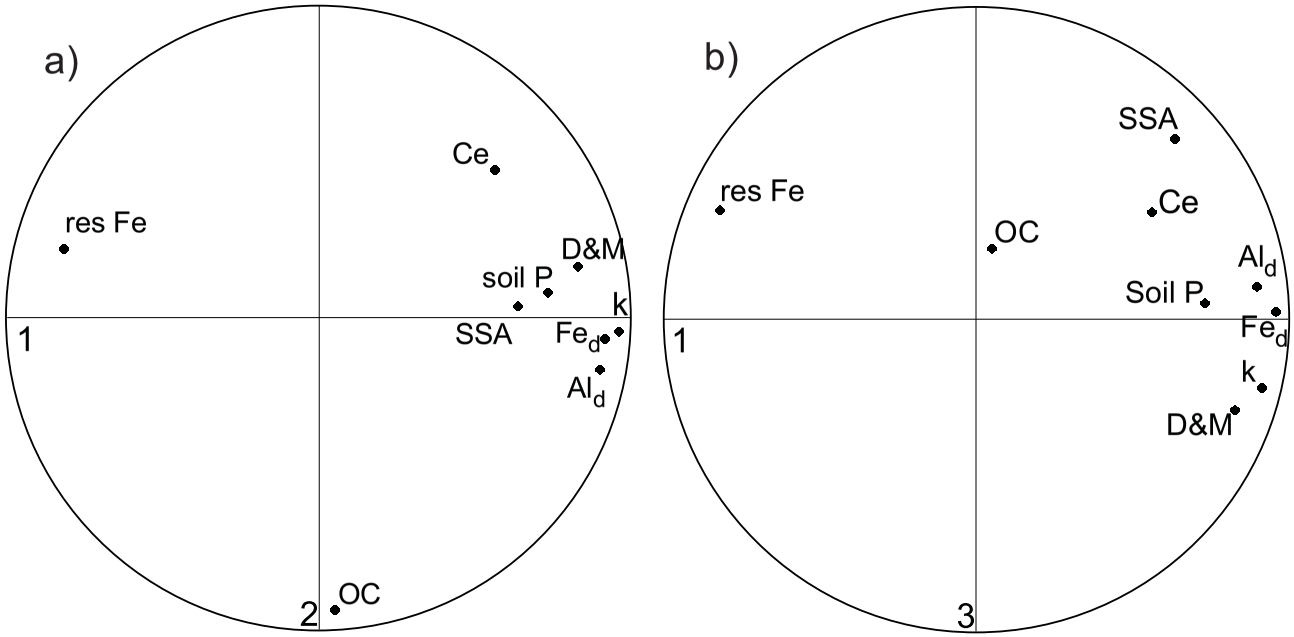
a)
Ce
res Fe
D&M
soil P
k
1
SSA
Fe$_d$
Al$_d$
2
OC
b)
SSA
res Fe
Ce
OC
Al$_d$
Soil P
Fe$_d$
1
k
D&M
3

Figure 7:

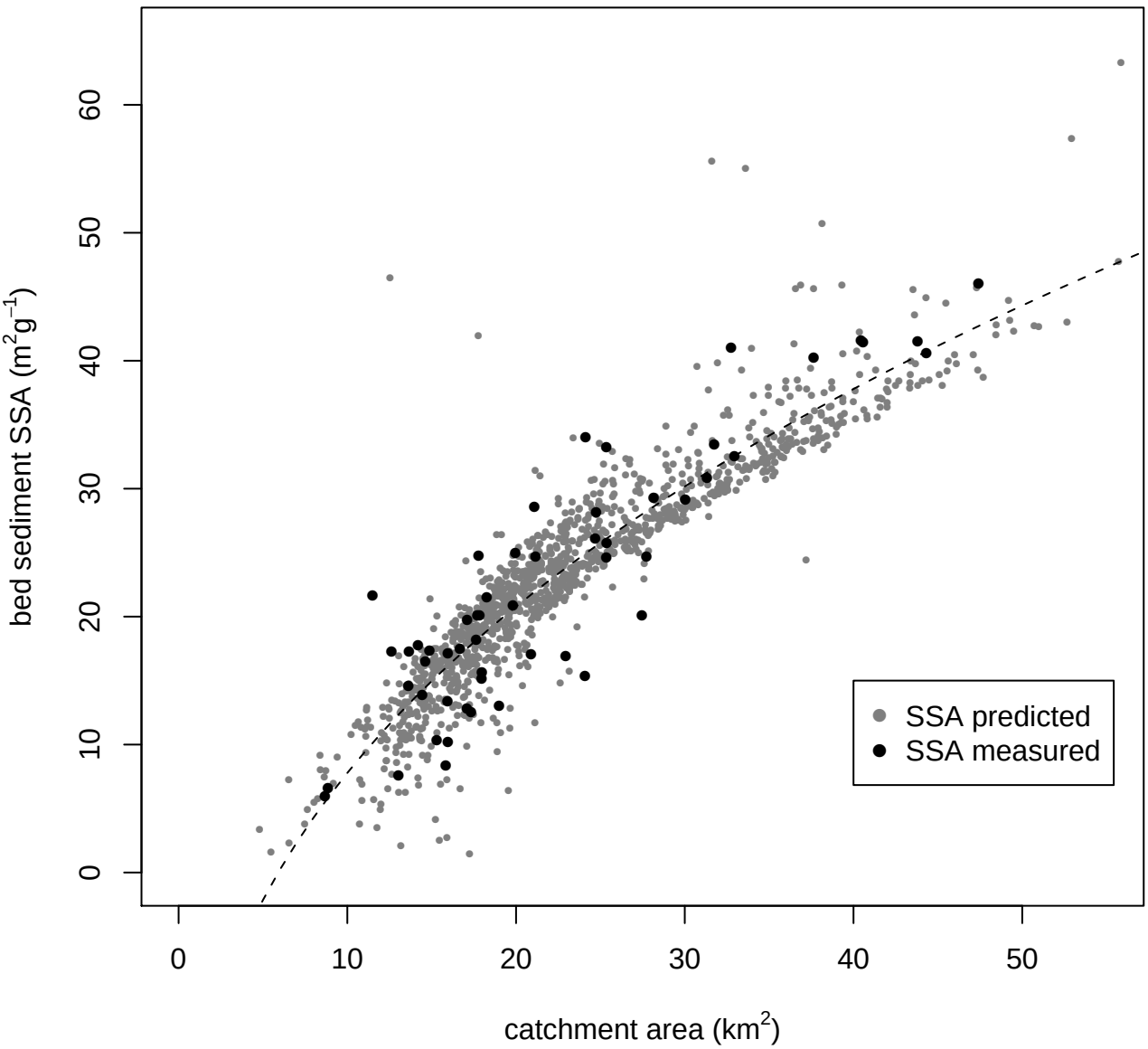

vs CA.pdf